

Phonon modes of monoclinic BiB_3O_6

A. Gössling^{*1}, T. Möller¹, W.-D. Stein¹, P. Becker³, L. Bohaty³, and M. Grüninger^{1,2}

¹ 2nd Physical Institute, University of Cologne, Zülpicher Str. 77, D-50937 Cologne, Germany

² 2nd Physical Institute, RWTH Aachen, Huygensweg, D-52056 Aachen, Germany

³ Institute of Crystallography, University of Cologne, Zülpicher Str. 49b, D-50674 Cologne, Germany

PACS 42.65.-k, 42.70.Mp, 63.20.-e, 63.20.Dj, 77.84.Fa

* E-mail: goessl@ph2.uni-koeln.de, Phone: +49 221 470 3770, Fax: +49 221 470 6708

We present a detailed study of the phonon modes of the monoclinic compound BiB_3O_6 based on polarized reflectivity measurements on single crystals.

The spectra are analysed by means of an extended Drude-Lorentz model, which allows us to resolve the modes of *A* and *B* symmetry.

1 Introduction Bismuth triborate, BiB_3O_6 , a polar, non-ferroelectric crystal has attracted interest in the last years due to its outstanding nonlinear optical properties [1-3]. The large optical nonlinearities open up a rich field of applications for frequency conversion of laser light via $\chi^{(2)}$ - and $\chi^{(3)}$ -processes, e.g. phase-matched second harmonic-generation (SHG) or optical parametric oscillation (OPO) and stimulated Raman scattering (SRS).

The exceptional optical non-linearities of BiB_3O_6 have been attributed to the bonds of the $[\text{BO}_3]$ units and to a lone-pair electron at the Bi atom [4]. Detailed studies of the lattice dynamics are required for a quantitative description of these bonds. Infrared (IR) and Raman studies of the phonons are only available at room temperature [3,5-8]. In particular, there is no polarization-dependent infrared study, but a polarization analysis is essential for an accurate determination of the phonon frequencies in monoclinic crystals [9]. In this letter we present a detailed investigation of the linear optical response of BiB_3O_6 in the phonon range for different polarizations at 20K and 300K. The data are analyzed in terms of an extended Drude-Lorentz model, which allows us to obtain the frequency, the damping, the strength and the orientation of the dipole moment of each phonon mode.

2 Experimental Large, right-handed single crystals of BiB_3O_6 were grown using the top seeded growth technique [8,10]. The crystal structure with space group symmetry $C2$ (C_2^3) ($a = 7.116(2)$ Å, $b = 4.993(2)$ Å, $c = 6.508(3)$ Å, $\beta = 105.62(3)^\circ$) consists of sheets of corner-

sharing $[\text{BO}_3]$ - and $[\text{BO}_4]$ -units in a ratio of 2:1, that are separated by sheets of six-fold coordinated Bi [11]. We performed reflectivity measurements at $T=20\text{K}$ and $T=300\text{K}$ in the spectral range of $50\text{-}8000\text{ cm}^{-1}$ at quasi-normal incidence. Using a Bruker IFS 66v/S Fourier-transform spectrometer the spectra were measured for different polarization angles on polished (010) and (100) surfaces of BiB_3O_6 . As a reference we used an Au mirror. The variation of the polarization angle was realized by rotating the polarizer.

3 Phonon modes The factor group analysis [12] yields the following irreducible representations for the space group $C2$:

$$\Gamma_{\text{BiB}_3\text{O}_6} = \Gamma_{C_2^3} = 14A + 16B \quad (1)$$

After subtraction of the three acoustic modes $A+2B$, our group theoretical analysis predicts 13*A* and 14*B* optical phonon modes. Due to the lack of a centre of inversion, *A* and *B* modes are active both in Raman [6,7] and in IR spectroscopy.

The linear dielectric response (without external magnetic field) of a monoclinic sample can be described by the tensor

$$\hat{\epsilon} = \begin{pmatrix} \epsilon_{xx} & 0 & \epsilon_{xz} \\ 0 & \epsilon_{yy} & 0 \\ \epsilon_{xz} & 0 & \epsilon_{zz} \end{pmatrix} \quad (2)$$

Note, that we assume $\mathbf{y} \parallel \mathbf{b}$, $\mathbf{z} \parallel \mathbf{c}$, and $\mathbf{x} \perp \mathbf{c}$ lying in the \mathbf{ac} plane, where \mathbf{a} , \mathbf{b} , and \mathbf{c} are the crystallographic axes (see inset of Fig. 1(a)). In order to determine the phonon modes we follow the procedure described in Ref. [9]. The tensor (2) can be decomposed into a scalar ε_b along the \mathbf{b} axis and a two-dimensional tensor $\hat{\varepsilon}_{ac}$ within the \mathbf{ac} plane. Since the \mathbf{b} axis is perpendicular to the \mathbf{ac} plane, the A -symmetry modes can be probed by measuring with the incident electric field \mathbf{E} parallel to the \mathbf{b} axis (e.g. on a (100) surface). Determining the B -symmetry modes requires the analysis of at least three polarization directions (with $\mathbf{E} \parallel \mathbf{ac}$ plane on a (010) surface) because the angle between the \mathbf{a} and the \mathbf{c} axis deviates from 90° . The orientation θ of the dipole moment within the \mathbf{ac} plane may be different for each B mode. Reflectivity spectra at $T=300\text{K}$ are shown for $\mathbf{E} \parallel \mathbf{b}$ in Fig. 1(d) and for $\mathbf{E} \parallel \mathbf{ac}$ in Fig. 1(a-c). The phonon spectra reach up to almost 1500 cm^{-1} due to the small mass of the B ions. Note, that only the room temperature data will be analyzed in detail as long as there are no fundamental differences between $T=20\text{K}$ and $T=300\text{K}$.

The dispersion of the scalar quantity ε_b is described by the Drude-Lorentz model, i.e. by a sum of oscillators, whereas the tensor $\hat{\varepsilon}_{ac}$ is described by an extended Drude-Lorentz model:

$$\varepsilon_b(\omega) = \varepsilon_{yy} = \varepsilon_b^\infty + \sum_{i,A} \frac{\omega_{p,i}^2}{\omega_{0,i}^2 - \omega^2 - i\gamma_i\omega} \quad (3)$$

$$\hat{\varepsilon}_{ac}(\omega) = \begin{pmatrix} \varepsilon_{xx} & \varepsilon_{xz} \\ \varepsilon_{xz} & \varepsilon_{zz} \end{pmatrix} = \hat{\varepsilon}_{ac}^\infty + \sum_{i,B} \frac{\omega_{p,i}^2}{\omega_{0,i}^2 - \omega^2 - i\gamma_i\omega} \times \begin{pmatrix} \cos^2 \theta_i & \sin \theta_i \cos \theta_i \\ \sin \theta_i \cos \theta_i & \sin^2 \theta_i \end{pmatrix}$$

Here, $\omega_{0,i}$ denotes the transverse frequency, $\omega_{p,i}$ the plasma frequency, γ_i the damping, and θ_i the angle between the dipole moment and the \mathbf{x} axis (in the case of the B -symmetry modes) of the i -th oscillator. The high-frequency dielectric constants are indicated by ε_b^∞ and ε_{ac}^∞ .

The reflectance for $\mathbf{E} \parallel \mathbf{b}$ (R_b) and $\mathbf{E} \parallel \mathbf{ac}$ (R_{ac}) can be obtained by using the Fresnel equations for normal incidence [9]:

$$R_b = \left| (1 - \sqrt{\varepsilon_b}) \cdot (1 + \sqrt{\varepsilon_b})^{-1} \right|^2 \quad (4)$$

$$R_{ac}(\chi) = \left| \left(\hat{\varepsilon}_{ac} - \sqrt{\hat{\varepsilon}_{ac}} \right) \cdot \left(\hat{\varepsilon}_{ac} + \sqrt{\hat{\varepsilon}_{ac}} \right)^{-1} \begin{pmatrix} \cos \chi \\ \sin \chi \end{pmatrix} \right|^2$$

In Eq. (4), χ denotes the angle between the polarization direction and the \mathbf{x} axis as shown in Fig. 1(a). In order to take the square root of a tensor, $\hat{\varepsilon}_{ac}$ first has to be rotated to a diagonal form, then the square root has to be taken for each element, and finally the resulting tensor is rotated back to its original basis.

The scalar ε_b is determined by fitting the single spectrum R_b , while $\hat{\varepsilon}_{ac}$ is determined by fitting $R_{ac}(\chi)$ for three

different values of χ simultaneously (we measured 14 different χ values). The fits yield an excellent description of the measured reflectivity. The fit parameters are listed in Tab. 1, and Fig. 1(e) shows the resulting optical

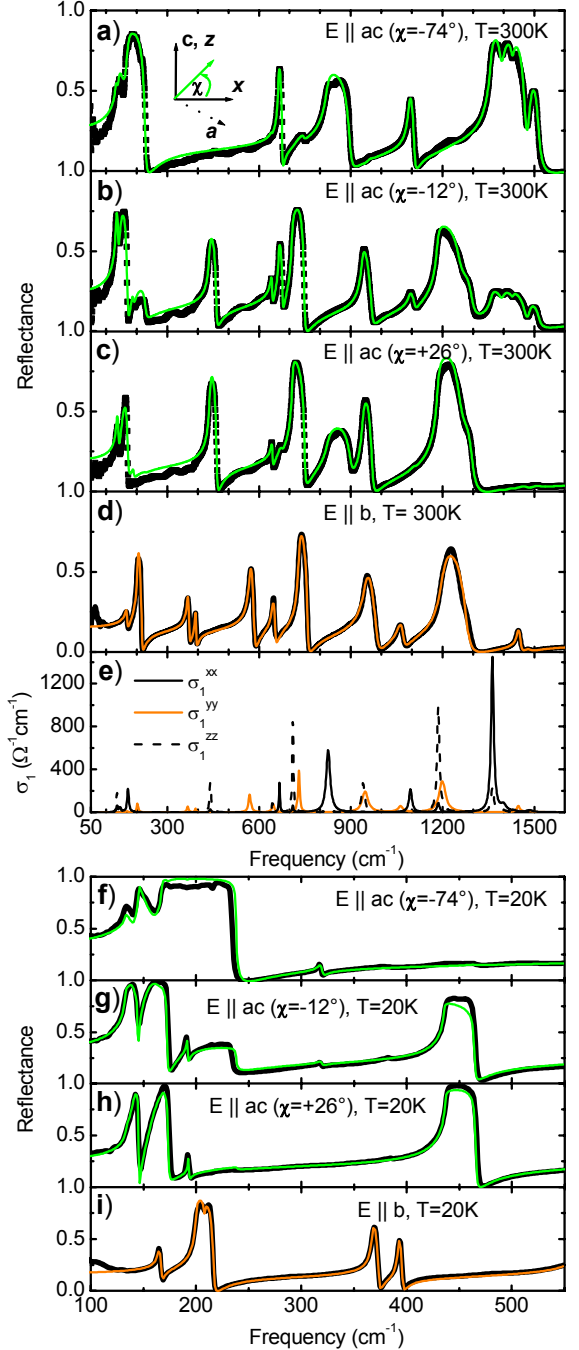


Figure 1 a) – c) Reflectivity spectra of BiB_3O_6 at $T=300\text{K}$ for $\mathbf{E} \parallel \mathbf{ac}$ -plane at different polarization angles χ (black) and fits using Eq. (4) (grey). d) Reflectivity at $T=300\text{K}$ for $\mathbf{E} \parallel \mathbf{b}$ (black), fits using Eq. (4). e) Optical conductivity corresponding to $\hat{\varepsilon}_{ac}$ (black) and ε_b (grey) for the fitted parameters. f-h) Reflectivity spectra of BiB_3O_6 at $T=20\text{K}$ for $\mathbf{E} \parallel \mathbf{ac}$ -plane at different polarization angles χ (black) and fits using Eq. (4) (grey). i) Reflectivity at $T=20\text{K}$ for $\mathbf{E} \parallel \mathbf{b}$ (black), fits using Eq. (4).

Table 1 Fit results for the reflectivity of BiB_3O_6 at $T=300\text{K}$ using Eq. (4). Here, ω_0 is the transverse frequency, ω_p the plasma frequency, γ the damping, θ the angle between the dipole moment and the x axis (in case of the B modes), and $S = \omega_p^2/\omega_0^2$ denotes the oscillator strength. The high-frequency dielectric constants at $T=300\text{K}$ are: $\varepsilon_{xx}^\infty = 3.5$, $\varepsilon_{yy}^\infty = 2.9$, $\varepsilon_{zz}^\infty = 3.3$ and $\varepsilon_{xz}^\infty = -0.3$.

B-Modes					A-Modes			
ω_0 (cm $^{-1}$)	ω_p (cm $^{-1}$)	γ (cm $^{-1}$)	θ (°)	S	ω_0 (cm $^{-1}$)	ω_p (cm $^{-1}$)	γ (cm $^{-1}$)	S
136	236	3.9	151	3.021	168	71	7.0	0.179
146	215	9.4	132	2.185	202	164	5.5	0.659
172	291	6.5	89	2.862	367	151	7.0	0.169
190	50	8.3	33	0.069	393	93	4.4	0.056
441	333	6.0	18	0.570	570	305	9.2	0.286
644	173	5.8	175	0.073	646	208	9.4	0.104
667	328	3.7	131	0.241	731	396	6.6	0.293
711	514	4.8	15	0.523	947	522	23	0.304
826	753	15.6	77	0.831	1062	256	20.0	0.058
940	448	12.1	6	0.227	1199	668	25.6	0.310
1095	415	11.5	111	0.143	1448	208	12.3	0.021
1187	792	9.7	16	0.445	1484	129	30.3	0.008
1363	1028	10.5	112	0.568				
1268	156	49.7	19	0.015				
1400	314	21.4	117	0.050				
1434	101	12.9	127	0.005				
1486	169	19.4	121	0.013				

conductivity of the diagonal elements of the dielectric tensor. In case of $\mathbf{E} \parallel \mathbf{b}$, where 13 A modes are expected, we find 11 strong IR modes and a series of weaker features. Most of the latter can be interpreted as multi-phonon excitations, e.g., a weak feature at 272 cm $^{-1}$, which can be attributed to an overtone of the B mode at 136 cm $^{-1}$ (note that $B \otimes B$ yields A symmetry).

In order to determine which of the weak features corresponds to a fundamental phonon mode, it is helpful to compare our data with Raman results [6,7]. In a recent room-temperature Raman study [6], 12 A modes have been observed. Ten modes are found both in the Raman and in the IR data (the transverse frequencies agree within a few wave numbers). Combined with the two additional Raman modes at 1294 and 1488 cm $^{-1}$ and with the strongly IR-active mode at 1062 cm $^{-1}$, we end up with 13 A modes, as expected. The Raman peak at 1488 cm $^{-1}$ corresponds to a weak IR feature. However, the Raman mode at 1294 cm $^{-1}$ was not found in Ref. [7]. Other features, which are weak in both spectroscopies, can be attributed to multi-phonon excitations (e.g. the peak at 272 cm $^{-1}$ discussed above) or to a polarizer leakage (e.g. the Raman mode at 443 cm $^{-1}$ corresponds to a strongly IR-active B mode).

In case of the ac plane, each phonon mode shows a different orientation θ of the dipole moment. This produces complex patterns in $R_{ac}(\chi)$ which can not be described by a simple Drude-Lorentz model. For the description of $R_{ac}(\chi)$ we used 17 oscillators, in contrast to the 14 B modes predicted. The use of four oscillators below 250 cm $^{-1}$ is based on the 20K data (see Fig. 1(f-g)). At high frequencies, the four modes at 1268, 1400, 1434, and 1486 cm $^{-1}$ are very

weak and show rather large values of the damping. These modes possibly have to be attributed to multi-phonon excitations. In case of the B modes the discrepancies between IR and Raman data are much larger because both transverse and longitudinal modes are observed in the Raman data [6,7]. In order to clarify this issue and to distinguish two-phonon excitations from the one-phonon modes detailed lattice-dynamical calculations are required.

4 Conclusion We have investigated a study of the phonon modes by reflectivity measurements. The data can be described excellently by means of an extended Drude-Lorentz model, which was used to determine the complete linear dielectric tensor in the frequency range of 50-8000 cm $^{-1}$.

References

- [1] H. Hellwig *et al.*, Solid State Commun. **109**, 249 (1999).
- [2] H. Hellwig *et al.*, J. Appl. Phys. **88**, 240 (2000).
- [3] A. A. Kaminskii *et al.*, Opt. Commun. **206**, 179 (2002).
- [4] D. Xue *et al.*, Phys. Stat. Sol. **176**, R1 (1999).
- [5] H. R. Xia *et al.*, J. Raman Spectrosc. **33**, 278 (2002);
- [6] X. Hu *et al.*, J. Appl. Phys. **97**, 033501 (2005).
- [7] D. Kasprowicz *et al.*, Cryst. Res. Technol. **40**, 459 (2005).
- [8] P. Becker *et al.*, Cryst. Res. Technol. **36**, 27 (2001).
- [9] A. B. Kuz'menko *et al.*, Phys. Rev. B **63**, 094303 (2001); A. B. Kuz'menko *et al.*, J. Phys. Condens. Matter **8**, 6199 (1996).
- [10] P. Becker *et al.*, Cryst. Res. Technol. **36**, 27 (2001).
- [11] R. Fröhlich *et al.*, Acta Cryst. **C40**, 343 (1984).
- [12] D. L. Rousseau *et al.*, J. Raman Spectrosc. **10**, 253 (1981).